Broken SU(3) symmetry in deformed even-even nuclei

N. Minkov,[1,*] S. B. Drenska,[1,†] P. P. Raychev,[1,2,‡] R. P. Roussev,[1,§] and Dennis Bonatsos[3,‖]
[1]*Institute for Nuclear Research and Nuclear Energy, 72 Tzarigrad Road, 1784 Sofia, Bulgaria*
[2]*Dipartimento di Scienze Fisiche, Università di Napoli ''Federico II,'' Mostra d' Oltremare Pad. 19, I-80185, Napoli, Italy*
[3]*Institute of Nuclear Physics, N.C.S.R. ''Demokritos,'' GR-15310 Aghia Paraskevi, Attiki, Greece*
(Received 10 September 1996)

A collective vector-boson model with broken SU(3) symmetry, in which the ground-state band and the lowest γ band belong to the same irreducible representation but are nondegenerate, is applied to several deformed even-even nuclei. The model description of ground and γ bands together with the corresponding $B(E2)$ transition probabilities is investigated within a broad range of SU(3) irreducible representations (λ,μ). The calculations show that the (λ,μ) characteristics of rotational nuclei depend to a great extent on the magnitude of the SU(3) splitting between the ground and γ bands. It is found that for weakly split spectra, the ground-γ band coupling scheme is realized relevantly within narrow regions of ''favored'' (λ,μ) multiplets, while in the cases of strong splitting a description in which the ground band is situated alone in an irreducible representation is favored. The obtained results are analyzed in terms of the band-mixing interactions. The possibility for a transition between the different collective SU(3) schemes is discussed.
[S0556-2813(97)02605-8]

PACS number(s): 21.60.Fw, 21.60.Ev, 27.70.+q, 27.90.+b

I. INTRODUCTION

The SU(3) symmetry group, which was introduced initially in nuclear theory as the symmetry group of s,d-shell nuclei [1], has also been given meaning in the framework of the dynamical symmetry (DS) concept [2–5]. Based on the DS concept, it has been supposed that the SU(3) symmetry is inherent for the well-deformed even-even nuclei, so that the low-lying ($L\leqslant 10$) collective states of these nuclei could be united into one or several SU(3) multiplets, labeled by the irreducible representations (irreps) (λ,μ) of the group SU(3) [6]. The collective rotational Hamiltonian reduces this symmetry to the rotational group O(3) and thus the energy spectrum of the nucleus is generated. In particular, it has been shown that in the rare-earth nuclei the ground-state band (gsb) and the first γ-excited band can be united into one split $(\lambda,2)$ multiplet appearing in a collective vector-boson scheme with broken SU(3) symmetry [6]. This scheme gives a satisfactory description of the energy levels and of the $B(E2)$ transition ratios within and between the bands. The success of the SU(3) scheme has inspired the extension of the concept of DS in nuclei to the noncompact group $Sp(6,\mathcal{R})$ [4,7–11], which contains SU(3) as a maximal compact subgroup. Alternatively, boson and fermion realizations of dynamical symmetries have been used in the interacting boson model (IBM) [having an overall U(6) symmetry] [12–15] and the fermion dynamical symmetry model [with $Sp(6,\mathcal{R})\times SU(2)$ and $SO(8)\times SU(2)$ overall symmetries] [17,18], respectively. In spite of the different realizations these extended algebraic schemes in the appropriate limit include SU(3) as a DS group which can be associated with the rotational limit of nuclear collective motion.

Various model realizations of a broken SU(3) symmetry have been applied to the nuclei of the rare earth and actinide regions by using appropriately selected SU(3) irreps. A microscopically justified one is the pseudo SU(3) model [having an SU(3) abstract symmetry], in which the SU(3) irrep (λ,μ) used for a given nucleus depends on the filling of the Nilsson pseudo-oscillator levels [19]. An alternative prescription for fixing the SU(3) quantum numbers λ and μ is used in [20,21] and is based on the original Elliott model [1]. In fact, the two schemes involve different SU(3) irreps for one the same nucleus, indicating that with respect to the abstract SU(3) symmetry (beyond the particular realization), the choice of an adequate (λ,μ) multiplet for the given nucleus is not unique. The above circumstance naturally leads to the question of whether the theoretically determined SU(3) irrep provides the best model description of the spectrum and how the pattern changes with varying λ and μ. It is therefore of interest to understand whether the appropriate irreps can be established directly on the basis of the available experimental data and whether they reflect the respective systematic behavior of the ground and γ band rotational structure of deformed nuclei.

In order to clarify these questions one should include in the study a large variety of (λ,μ) multiplets and try to determine the ones favored by comparison to the experimental data. Such an approach can be naturally applied in the framework of the vector-boson model scheme [6,22,23], in which the possible SU(3) multiplets are not restricted by the underlying theory. This suggests that the SU(3) quantum numbers λ and μ are external parameters of the model scheme, allowing one to vary them so as to obtain the SU(3) irreps in which the experimental energies and transition probabilities are reproduced most accurately. Once such ''favored'' SU(3) irreps are found, one can apply them to the analysis of the collective dynamical characteristics of nuclei as well as to

*Electronic address: nminkov@inrne.acad.bg
†Electronic address: sdren@inrne.acad.bg
‡Electronic address: raychev@bgcict.acad.bg
§Electronic address: rousev@inrne.acad.bg
‖Electronic address: bonat@cyclades.nrcps.ariadne-t.gr

the discussion of the physical meaning of the vector-boson scheme.

An important characteristic of the SU(3) multiplets is the energy splitting of the even angular momentum states into the respective states belonging to the gsb and the γ band. The splitting is due to the reduction of the SU(3) symmetry in the nucleus and characterizes the mutual disposition of the two rotational bands within the multiplet. Thus one could expect that the possible existence of favored SU(3) irreps will depend on the energy splitting as well as on the intrinsic rotational structure of the bands.

In this paper we report a global study of the broken SU(3) symmetry in deformed even-even nuclei, implemented through the use of the vector-boson formalism [6,22,23]. Motivated by the above considerations, we suppose that for a given rotational nucleus the physically significant features of this symmetry should be sought in certain regions of SU(3) irreps instead of a single fixed irrep. The aims of this work are concentrated on the following items.

(i) To study whether in the framework of the vector-boson scheme the available experimental information on the energy levels and transition probabilities could be used to estimate the SU(3) symmetry characteristics of the nucleus, in particular to outline the physically favored regions in the (λ,μ) plane.

(ii) To study how the picture changes in the various nuclei, where different energy splittings between the ground-state band and the first γ-excited band are observed, and if the SU(3) nuclei could be systematized accordingly.

(iii) To investigate the principal limits of applicability of the SU(3) symmetry in nuclei by analyzing the band-mixing interactions in terms of the vector-boson formalism.

We have considered eight rare-earth nuclei (^{164}Dy, $^{164-168}$Er, ^{168,172}Yb, ^{176,178}Hf) and one actinide nucleus (^{238}U) for which the model descriptions of the gsb and γ-band energy levels and the concomitant $B(E2)$ transition ratios have been evaluated (in the form of root-mean-square fits) in SU(3) irreps within the range $10\leqslant\lambda\leqslant160$ and $2\leqslant\mu\leqslant8$. These nuclei represent regions of SU(3) spectra with different magnitudes of energy splitting between the gsb and the first γ-band. Though some other nuclei could also be included in the study, we shall see that the considered ones are sufficient to trace the most important features of SU(3) DS in collective rotational regions.

A few comments and clarifications are in place at this point.

(i) The vector bosons used in the vector-boson model [6] do not possess any underlying physical content, in contrast to the bosons used in the interacting boson model (IBM) [16], which are understood as correlated fermion pairs (see [24] and references therein). The vector bosons are the building blocks of the vector-boson model and the broken SU(3) symmetry, which do have a physical content, as it will be seen later. There is no contradiction between the last two statements. The situation is similar to that of the Schwinger boson realization of SU(2) [25–27]: The bosons used for the realization do not bear any particular physical content themselves, but the SU(2) operators built out of them are the physically meaningful angular-momentum operators.

(ii) The SU(3) symmetry discussed in this paper is a broken SU(3) symmetry, in which the ground-state band and the lowest γ band belong to the same irrep but are nondegenerate. The lowest β band is not contained in the same irrep. The situation differs drastically from that of the SU(3) limit of IBM [14], in which a pure SU(3) symmetry is the starting point, the ground-state band sitting alone in an irrep, with the lowest γ and β bands belonging to the next irrep and being degenerate. The degeneracy of the even angular-momentum levels of the lowest β and γ bands is a hallmark of the SU(3) symmetry of IBM.

In Sec. II the vector-boson scheme, which in the lowest SU(3) irreps $(\lambda,2)$ allows one to derive analytical expressions for the energy levels and transition probabilities [6], is extended for calculations in the higher irreps with $\mu>2$. In Sec. III we describe the numerical procedure and estimate the significance of the Hamiltonian parameters for the model description. The obtained results and the corresponding theoretical analysis are presented in Sec. IV while in Sec. V the conclusions are given.

II. THE VECTOR-BOSON MODEL WITH A BROKEN SU(3) SYMMETRY

A. Basis and Hamiltonian

The present realization of the SU(3) dynamical symmetry is founded on the assumption that the low-lying collective states of the nuclear system can be constructed effectively with the use of two distinct kinds of vector bosons, whose creation operators ξ^+ and η^+ are O(3) vectors and in addition transform according to two independent SU(3) irreps of the type $(\lambda,\mu)=(1,0)$. The vector bosons are interpreted as the quanta of the elementary collective excitations of the nucleus. The basic states corresponding to the reduction chain

$$\mathrm{SU}(3)\supset\mathrm{O}(3)\supset\mathrm{O}(2) \tag{1}$$

can be constructed as polynomials in the vectors ξ^+_ν and $\eta^+_\nu(\nu=1,0,-1)$ acting on the vacuum state. The set of these states, usually denoted as

$$\left|\begin{matrix}(\lambda,\mu)\\ \alpha,L,M\end{matrix}\right\rangle, \tag{2}$$

is known as the basis of Bargmann and Moshinsky [28,29]. Since the chain (1) is not canonical, i.e., in a given SU(3) irrep (λ,μ) more than one O(3) irreps (L,M) appear, an additional quantum number α is introduced in order to distinguish the states with equal angular momenta L. The quantum number α is related to the Elliott quantum number K as $\alpha=(\mu-K)/2$ [22]. The basis vectors (2) are not orthogonal with respect to α and could be orthonormalized by means of the Hilbert-Schmidt procedure [22]. For a given L, the quantum number α runs over all integers in the interval [22,29]

$$\max\{0,\tfrac{1}{2}(\mu-L)\}\leqslant\alpha\leqslant\min\{\tfrac{1}{2}(\mu-\beta),\tfrac{1}{2}(\lambda+\mu-L-\beta)\}, \tag{3}$$

where

$$\beta=\begin{cases}0, & \lambda+\mu-L \ \text{ even},\\ 1, & \lambda+\mu-L \ \text{ odd}\ .\end{cases} \tag{4}$$

The values $\{\alpha_j\}_{j=1-d_L}$ with $\alpha_j<\alpha_{j+1}$ determined in Eq. (3) label the different bands in which the angular momentum L appears and d_L is the multiplicity of the O(3) irrep (L,M) in the decomposition (1). Thus, in the case of the $(\lambda,\mu\geqslant 4)$ multiplet $(\lambda>\mu;\lambda,\mu$ even), the number α_{d_L} labels the ground state band with $L=0,2,4,\ldots,\lambda$; α_{d_L-1} labels the γ band with $L=2,3,\ldots,\lambda+2$; α_{d_L-2} corresponds to a band with $L=4,5,\ldots,\lambda+4$, etc. In the case $(\lambda,2)$ the above scheme provides only two bands, the gsb and the γ band, labeled by the quantum numbers $\alpha_2=1$ and $\alpha_1=0$, respectively.

The collective Hamiltonian of the vector-boson scheme is based on the experimentally supported view that in deformed even-even nuclei the nuclear effective interaction is dominated by the collective quadrupole mode. Thus, it is assumed that the basic collective properties of these nuclei are determined by their angular and quadrupole momenta, which are naturally incorporated within the framework of the SU(3) DS. The effective SU(3) symmetry-breaking Hamiltonian which should be an O(3) invariant [30,31] is constructed by using three basic O(3) scalars as follows [23]:

$$V=g_1L^2+g_2L\cdot Q\cdot L+g_3A^+A, \tag{5}$$

where g_1, g_2, and g_3 are the parameters of the model; L and Q are the angular-momentum and quadrupole operators, respectively, in the vector-boson realization:

$$L_m=-\sqrt{2}\sum_{\mu,\nu} C^{1m}_{1\mu1\nu}(\xi^+_\mu\xi_\nu+\eta^+_\mu\eta_\nu),\quad m=0,\pm1, \tag{6}$$

$$Q_k=\sqrt{6}\sum_{\mu,\nu} C^{2k}_{1\mu1\nu}(\xi^+_\mu\xi_\nu+\eta^+_\mu\eta_\nu),\quad k=0,\pm1,\pm2, \tag{7}$$

with $C^{LM}_{lmlm'}$ denoting the Clebsch-Gordan coefficients; the term A^+A introduced originally in [32] is constructed by the operator

$$A^+=\boldsymbol{\xi}^{+2}\boldsymbol{\eta}^{+2}-(\boldsymbol{\xi}^+\cdot\boldsymbol{\eta}^+)^2 \tag{8}$$

and its Hermitian conjugate A. The physical content of A^+A is discussed in [23] by assuming that the vectors $\boldsymbol{\xi}^+$ and $\boldsymbol{\eta}^+$ form a ''pseudospin'' doublet. This allows one to label the SU(3) multiplets by the numbers (N,T) ($N=0,1,2,\ldots$; $T=\frac{1}{2}N,\frac{1}{2}N-1,\frac{1}{2}N-2,\ldots$), which are related to (λ,μ) as

$$N=\lambda+2\mu,\quad T+\lambda/2. \tag{9}$$

The number N corresponds to the number of vector bosons (interpreted as related to the number of excitation quanta in the nucleus) and T is the ''pseudospin'' of the system of N vector bosons. It has been shown that in these terms the operator A^+ can be considered as a creation operator of four particles with $L=0$ and $T=0$. In this way the operator A^+A has been interpreted as the number operator of ''α-like'' configurations in nuclei.

B. Energies and $B(E2)$ transition probabilities

The eigenstate of the effective Hamiltonian (5) with given angular momentum L and energy ω^L can be constructed from the highest-weight (hw) basis states (with $M=L$) as follows:

$$\left|\begin{matrix}(\lambda,\mu)\\ \omega^L,L,L\end{matrix}\right\rangle=\sum_{j=1}^{d_L} C^L_{\omega,j}\left|\begin{matrix}(\lambda,\mu)\\ \alpha_j,L,L\end{matrix}\right\rangle. \tag{10}$$

Then the standard problem for eigenfunctions and eigenvalues reduces to the following homogeneous set of equations (written in matrix form) for the coefficients $C^L_{\omega,j}$:

$$(V_{j,j'}-\omega^L\delta_{j,j'})(C^L_{\omega,j'})=0,\quad j,j'=1\div d_L, \tag{11}$$

where

$$V_{j,j'}\equiv\left\langle\begin{matrix}(\lambda,\mu)\\ \alpha_j,L,L\end{matrix}\right|V\left|\begin{matrix}(\lambda,\mu)\\ \alpha_{j'},L,L\end{matrix}\right\rangle$$

are the matrix elements of the Hamiltonian (5) between the hw basis states and $(C^L_{\omega,j'})$ is a vector column. The eigenvalues ω^L_i, $i=1-d_L$ (with $\omega_i<\omega_{i+1}$) are determined by

$$\det(V_{j,j'}-\omega^L\delta_{j,j'})=0. \tag{12}$$

In the low-dimensional cases with $\mu=2,4$, where $d_L=2,3$, Eq. (12) can be solved analytically [6], while in the cases with $\mu>4$ one should find ω^L_i by numerical diagonalization of the matrix $(V_{j,j'})$. We remark that the interaction V mixes only basis states with neighboring values of the quantum number α so that the matrix $(V_{j,j'})$ is tridiagonal. The analytical form of the matrix elements of the operators $L\cdot Q\cdot L$ and A^+A is given in Table I. Since the basis of Bargmann and Moshinsky is nonorthogonal, the matrix $(V_{j,j'})$ is not Hermitian. This fact does not affect the obtaining of real eigenvalues when the model parameters g_1, g_2, and g_3 are real. After obtaining the eigenvalues ω^L_i, one is able to derive the corresponding coefficients $C^L_{i,j}\equiv C^L_{\omega_i,j}$, $i,j=1-d_L$. Below we show how this can be done easily even in the cases with large dimension. For a given eigenvalue ω^L_i we introduce the coefficients

$$h_{i,j}=C^L_{i,j}/C^L_{i,1},\quad j=1-d_L, \tag{13}$$

with $h_{i,1}=1$. Thus the set (11) is reduced to a nonhomogeneous set of d_L-1 equations for the coefficients $h_{i,j}$, $j=2-d_L$. Then using the tridiagonal form of the matrix $(V_{j,j'})$, we derive the solution of this set (for arbitrary d_L) in the following recursive form:

$$h_{i,j}=-\{V_{j-1,j-2}h_{i,j-2}+(V_{j-1,j-1}-\omega^L_i)h_{i,j-1}\}/V_{j-1,j},\quad j=3-d_L, \tag{14}$$

with

$$h_{i,2}=-(V_{1,1}-\omega^L_i)/V_{1,2}. \tag{15}$$

After obtaining the coefficients $h_{i,j}$ and using the orthonormalization of the eigenfunction (10) we find the first coefficient $C^L_{i,1}$:

TABLE I. Matrix elements of the operators $L\cdot Q\cdot L$ and A^+A between the basis states of Eq. (2).

s	$\left\langle \begin{matrix}(\lambda,\mu)\\ \alpha+s,L,L\end{matrix}\right\vert L\cdot Q\cdot L\left\vert \begin{matrix}(\lambda,\mu)\\ \alpha,L,L\end{matrix}\right\rangle$
0	$4\alpha[L(L+1)-3(L+2\alpha-\mu+\beta)^2]$ $-2(\lambda+\mu-L-\beta-2\alpha)[L(L+1)-3(\mu-2\alpha)^2]$ $-(L-2\mu+4\alpha+\beta)(2L+3)(L+1+3\beta)$
1	$-6(\lambda+\mu-L-\beta-2\alpha)(\mu-2\alpha-\beta)(\mu-2\alpha-\beta-1)$
-1	$12\alpha(L+2\alpha-\mu)(L+2\alpha-\mu-1)$

s	$\left\langle \begin{matrix}(\lambda,\mu)\\ \alpha+s,L,L\end{matrix}\right\vert A^+A\left\vert \begin{matrix}(\lambda,\mu)\\ \alpha,L,L\end{matrix}\right\rangle$
0	$-\frac{4}{3}\,\alpha\{(\alpha-1)[L(L+1)-3(L+2\alpha-\mu+\beta)^2]$ $-(\lambda+\mu-L-\beta-2\alpha)[L(L+1)-3(\mu-2\alpha)^2]$ $-\frac{1}{2}\,(L-2\mu+4\alpha+\beta)(2L+3)(L+1+3\beta)\}$ $+\sum_{k=1}^{\alpha}(\lambda+2\mu+3-4k)[(\lambda+2\mu+3-4k)^2+3-\frac{3}{4}\,L(L+1)-\lambda(\lambda+2)]$
1	$(\lambda+\mu-L-\beta-2\alpha)(\mu-2\alpha-\beta)(\mu-2\alpha-\beta-1)(L+\lambda+\mu+2\alpha+\beta+2)$
-1	$-4\alpha(\alpha-1)(L+2\alpha-\mu)(L+2\alpha-\mu-1)$

$$C^L_{i,1}=\left\langle 2\sum_{j=1}^{d_L}\sum_{j'=1}^{j} h_{i,j}h_{i,j'}\left\langle \begin{matrix}(\lambda,\mu)\\ \alpha_j,L,L\end{matrix}\middle|\begin{matrix}(\lambda,\mu)\\ \alpha_{j'},L,L\end{matrix}\right\rangle -\sum_{j=1}^{d_L} h^2_{i,j}\left\langle \begin{matrix}(\lambda,\mu)\\ \alpha_j,L,L\end{matrix}\middle|\begin{matrix}(\lambda,\mu)\\ \alpha_j,L,L\end{matrix}\right\rangle\right\rangle^{-1/2}, \tag{16}$$

where the analytical form of the overlap integrals

$$\left\langle \begin{matrix}(\lambda,\mu)\\ \alpha_j,L,L\end{matrix}\middle|\begin{matrix}(\lambda,\mu)\\ \alpha_{j'},L,L\end{matrix}\right\rangle$$

is given in [22]. The remaining coefficients $C^L_{i,j}$, $j=2-d_L$ are then determined through Eq. (13). In such a way, applying the above procedure for all eigenvalues ω^L_i, $i=1-d_L$ we obtain the matrix $(C^L_{i,j})$ which transforms the space of the basis functions

$$\left\vert \begin{matrix}(\lambda,\mu)\\ \alpha_j,L,L\end{matrix}\right\rangle$$

into the space of the physical states (with determined energies)

$$\left\vert \begin{matrix}(\lambda,\mu)\\ \omega^L,L,L\end{matrix}\right\rangle.$$

In order to obtain the $B(E2)$ transition probabilities in a given multiplet (λ,μ) one can use the action of the operator Q_0 (7) on the hw basis state

$$Q_0\left\vert \begin{matrix}(\lambda,\mu)\\ \alpha,L,L\end{matrix}\right\rangle=\sum_{\substack{k=0,1,2\\ s=0,\pm1}} a^k_s\left\vert \begin{matrix}(\lambda,\mu)\\ \alpha+s,L+k,L\end{matrix}\right\rangle, \tag{17}$$

where the coefficients a^k_s are given in [23]. Then the matrix elements of Q_0 between the states with determined energy values (10) can be derived in the form

$$\left\langle \begin{matrix}(\lambda,\mu)\\ \omega^{L+k}_{i'},L+k,L\end{matrix}\middle|Q_0\middle|\begin{matrix}(\lambda,\mu)\\ \omega^L_i,L,L\end{matrix}\right\rangle=\sum_{j=1}^{d_L} C^L_{i,j}\sum_{s=0,\pm1} a^k_s R^{L+k}_{\alpha_j+s,i'}, \tag{18}$$

where i, i' and k take the values $i=1-d_L$; $i'=1-d_{L+k}$, and $k=0,1,2$; the matrix C^L is determined for the states with angular momentum L by Eqs. (13)–(16) and the matrix R^L is defined as $R^L=(C^L)^{-1}$. The most general form of the $B(E2)$ reduced transition probability with $\Delta L=k$ between the level corresponding to the eigenvalue ω^L_i and the level corresponding to $\omega^{L+k}_{i'}$ is

$$B(E2;\omega^L_i\rightarrow\omega^{L+k}_{i'})=\frac{1}{2L+1}\begin{pmatrix} L+k & 2 & L\\ -L & 0 & L\end{pmatrix}^{-2}\times\left\vert\left\langle \begin{matrix}(\lambda,\mu)\\ \omega^{L+k}_{i'},L+k,L\end{matrix}\middle|Q_0\middle|\begin{matrix}(\lambda,\mu)\\ \omega^L_i,L,L\end{matrix}\right\rangle\right\vert^2. \tag{19}$$

III. PARAMETERS AND NUMERICAL CALCULATIONS

We have realized numerically the general model scheme, given in the previous section. Thus, in a particular (λ,μ) multiplet ($\lambda>\mu$; λ, μ even) we diagonalize the matrix $(V_{j,j'})$ for the various angular momenta L. The gsb and γ-band levels with even L are then determined as $E_g(L)=\omega^L_1-\omega^0$ and $E_\gamma(L)=\omega^L_2-\omega^0$, respectively, where ω^L_1 and ω^L_2 are the lowest and the next larger Hamiltonian eigenvalues, respectively, and $\omega^0=g_3\mu^2(\lambda+\mu+1)^2$ is the zero-level eigenvalue. The γ-band energies with odd L are determined as $E_\gamma(L)=\omega^L_1-\omega^0$.

By using Eq. (19) for the obtained energy levels, we calculated the following $B(E2)$ interband transition ratios:

$$R_1(L)=\frac{B(E2;L_\gamma\rightarrow L_g)}{B[E2;L_\gamma\rightarrow(L-2)_g]},\quad L\ \text{even},$$

$$R_2(L)=\frac{B[E2;L_\gamma\rightarrow(L+2)_g]}{B(E2;L_\gamma\rightarrow L_g)},\quad L\ \text{even},$$

$$R_3(L)=\frac{B[E2;L_\gamma\rightarrow(L+1)_g]}{B[E2;L_\gamma\rightarrow(L-1)_g]},\quad L\ \text{odd},\tag{20}$$

and the gsb intraband ratios:

$$R_4(L)=\frac{B[E2;L_g\rightarrow(L-2)_g]}{B[E2;(L-2)_g\rightarrow(L-4)_g]},\tag{21}$$

where the indices g and γ label the gsb and the γ-band levels, respectively. In the actinide nuclei the experimental information on the interband transitions does not suffice to provide any fits, so that in these cases (in particular in ^{238}U) we consider only the intraband ratios (21).

At this point it is important to estimate the significance of the Hamiltonian parameters g_1, g_2, and g_3 for the model calculations. The first parameter, g_1, applies only to the diagonal matrix elements of the Hamiltonian and contributes only to the rotational part of the energy levels. The second and third terms, $L\cdot Q\cdot L$ and A^+A, have diagonal as well as nondiagonal matrix elements (see Table I), so that the parameters g_2 and g_3 are significant for the rotational structure of the levels as well as for the band-mixing interaction. On the other hand, the diagonal contribution of the latter terms is responsible for the energy differences between the levels with equal angular momenta and different quantum numbers α, which means that g_2 and g_3 are also significant for the splitting of the SU(3) multiplet.

In order to illustrate the above considerations, we refer to the particular case of the (λ,2) irreps. In a given (λ,2) irrep and for a given L the general form of the Hamiltonian matrix elements is

$$V_{i,j}=\langle\alpha_i|V|\alpha_j\rangle=g_1\langle\alpha_i|L^2|\alpha_j\rangle+g_2\langle\alpha_i|L\cdot Q\cdot L|\alpha_j\rangle+g_3\langle\alpha_i|A^+A|\alpha_j\rangle,\tag{22}$$

where the indices $i,j=1,2$ label the two α values: $\alpha_1=0$ and $\alpha_2=1$. Thus we have

$$V_{1,1}=\langle\alpha=0|V|\alpha=0\rangle,\tag{23}$$

$$V_{2,2}=\langle\alpha=1|v|\alpha=1\rangle,\tag{24}$$

$$V_{1,2}=\langle\alpha=0|V|\alpha=1\rangle,\tag{25}$$

$$V_{2,1}=\langle\alpha=1|V|\alpha=0\rangle.\tag{26}$$

Hence for the calculation of $V_{1,1}$ one needs from Table I the values $\alpha=0$, $s=0$; for $V_{2,2}$ one needs $\alpha=1$, $s=0$; for $V_{1,2}$ one needs $\alpha=1$, $s=-1$; for $V_{2,1}$ one needs $\alpha=0$, $s=1$.

In this way one can easily see that in the case of L being even [in which $\beta=0$ according to Eq. (4)] the diagonal terms of the Hamiltonian are (see Table I).

$$V_{1,1}=g_1L(L+1)-g_2\{(2\lambda+5)[L(L+1)-12]-6L(L-1)\},\tag{27}$$

$$V_{2,2}=g_1L(L+1)-g_2\{(2\lambda+5)L(L+1)-6L(L-1)\}+g_3[4(\lambda+3)^2-2L(L+1)],\tag{28}$$

while the off-diagonal ones are

$$V_{1,2}=g_2 12L(L-1),\tag{29}$$

$$V_{2,1}=g_2 6[-(2\lambda+5)+(2L+1)]+g_3 2(\lambda+L+4)(\lambda-L+2).\tag{30}$$

In the case of odd L [in which $\beta=1$ according to Eq. (4)] one finds (see Table I)

$$V_{1,1}=g_1L(L+1)-g_2(2\lambda+5)[L(L+1)-12].\tag{31}$$

The gsb and γ-band energy levels are then obtained in the form

$$E_g(L)=AL(L+1)-B\{\sqrt{[1+CL(L+1)]^2+Df(L)}-1\},\tag{32}$$

$$E_\gamma(L^{\text{even}})=2B+AL(L+1)+B\{\sqrt{[1+CL(L+1)]^2+Df(L)}-1\},\tag{33}$$

$$E_\gamma(L^{\text{odd}})=2B+AL(L+1),\tag{34}$$

where

$$A=g_1-(2\lambda+5)g_2-g_3,\tag{35}$$

$$B=6(2\lambda+5)g_2-2(\lambda+3)^2g_3,\tag{36}$$

$$C=\frac{1}{6(2\lambda+5)}\frac{g_3}{g_2},\tag{37}$$

$$D=\frac{12}{B^2}[3g_2^2-g_2g_3],\tag{38}$$

and

$$f(L)=L(L-1)(L+1)(L+2).\tag{39}$$

These levels have been obtained with respect to the zero-level eigenvalue $\omega^0=4g_3(\lambda+3)^2$, as explained in the beginning of Sec. III.

The linear combination of parameters A could be interpreted as the inertia term, corresponding to the nonmixed part of the energy levels. The quantity $2B$ has the meaning of the γ-band bandhead, while C and D contribute to the mixed part of the energy levels. Note that $f(L)$ coincides with the square of the $\Delta K=2$ band-mixing term of the Bohr-Mottelson model [57].

The above expressions indicate two specific features of the present model in the (λ,2) case.

(i) The odd γ-band levels, which in this case are not mixed with any other levels, exhibit a rigid rotor behavior.

(ii) In the particular case $g_3/g_2=3$ the quantity D vanishes, so that despite the splitting both the gsb and the γ band contain only terms which are powers of $L(L+1)$.

It is also useful to rewrite Eqs. (32) and (33) in the form

$$E_\nu(L)=\left(\frac{1}{2\mathcal{J}_0}+\frac{1}{2\mathcal{J}_L}\right)L(L+1)+\frac{1}{2\mathcal{J}_L}\frac{D}{C}f(L)+\frac{C}{2\mathcal{J}_L}L^2(L+1)^2, \tag{40}$$

where L is even, $\upsilon=g,\gamma$ and

$$\mathcal{J}_0=\frac{1}{2A}, \tag{41}$$

$$\mathcal{J}_L=\frac{1}{BC}\left(1+\frac{1}{2B}\Delta E(L)\right), \tag{42}$$

with

$$\Delta E(L)=E_\nu(L)-\frac{1}{2\mathcal{J}_0}L(L+1). \tag{43}$$

The first term in Eq. (40) corresponds to the energy of a nonrigid rotor, the moment of inertia of which is angular-momentum dependent. This dependence is similar to the one occurring in the variable moment of inertia (VMI) model [33]. The other (higher-order) terms also depend on the angular momentum through $\Delta E(L)$. In such a way Eq. (40) indicates that the influence of the Hamiltonian parameters on the energy characteristics of the model is essentially nonlinear.

Now, regarding the transition probabilities, we consider the recursive equations (14) and (15). We remark that since g_1 enters only in the diagonal part of the Hamiltonian, the subtraction $(V_{j-1,j-1}-\omega_i^L)$ in Eq. (14) eliminates its contribution to the determination of the eigenfunctions and consequently of the transition probabilities. More precisely, the contribution of the diagonal matrix elements to the eigenvalues is not affected by the diagonalization procedure. Also one can deduce easily that the eigenvalues, as solutions of Eq. (12), should be homogeneous functions of the parameters g_2 and g_3, so that after dividing both the numerators and the denominators of Eqs. (14) and (15) by g_2 (or g_3) one concludes that the wave-function coefficients and the transition probabilities should depend only on the ratio g_3/g_2 (or g_2/g_3). Thus, while the energy description requires appropriate values of all Hamiltonian parameters, the inclusion of the transition probabilities in the fitting procedure only fixes the ratio g_3/g_2 (or g_2/g_3). We also remark that if one sets g_3 (or g_2) equal to zero, which means to neglect the term A^+A (or $L\cdot Q\cdot L$), the transition probabilities will obtain some constant (nonadjustable) values. It follows that both symmetry-breaking terms are necessary for a reasonable description of the $B(E2)$ transition probabilities within the present SU(3) scheme.

For obtaining the model description in a given SU(3) irrep (λ,μ) we have adjusted the Hamiltonian parameters to the low-lying experimental gsb and γ-band energy levels (up to $L=8-10$) and to the available transition ratios between them. This is implemented by using the χ^2 minimization procedure based on the direction set (Powell's) method (DSM) [34]. The quality of the energy fits is measured by

$$\sigma_E=\sqrt{(1/n_E)\sum_{L,\nu}[E_\nu^{\rm th}(L)-E_\nu^{\rm expt}(L)]^2}, \tag{44}$$

which is the standard energy rms deviation with n_E being equal to the number of the levels used in the fit and $\nu=g,\gamma$ labeling the gsb and the γ-band levels, respectively. By analogy, the quality of the fit of the transition ratios is measured by

$$\sigma_B=\sqrt{(1/n_B)\sum_{L,\tau}[R_\tau^{\rm th}(L)-R_\tau^{\rm expt}(L)]^2}, \tag{45}$$

which is the rms deviation of the transition ratios of Eq. (20), with n_B being the number of the ratios used in the fit and $\tau=1,2,3,4$ labeling the different types of ratios defined in Eqs. (20) and (21). The experimental data on energy levels are taken from [35]. The data on electromagnetic transitions are taken as follows: ^{164}Dy [36–38], ^{164}Er [38,39], ^{166}Er [40–42], ^{168}Er [43–45], ^{168}Yb [45,46], ^{172}Yb [47–49], ^{176}Hf [50,51], ^{178}Hf [52,53], ^{238}U [54]. In this method weight factors are used in order to account for the different orders of magnitude of the energy levels and the transition ratios, which are fitted simultaneously. The direction set (Powell's) method (DSM) [34] used here does not involve any computation of the gradient of any function and is directly applicable to the numerical realization of the present model. In addition we have tested an alternative fitting procedure involving numerical derivation, in which the differences between the model predictions and the experimental data are minimized with the use of an iterational procedure of Gauss-Newton (GN) type [55]. In this method the energy levels and the transition ratios are again fitted simultaneously, but this time with equal (unit) weight factors. In this way we have found that the independent application of both fitting procedures, DSM and GN, in a given SU(3) irrep (λ,μ) leads to the same values for the Hamiltonian parameters. This fact shows that the theoretical scheme developed in the previous section provides a numerically stable model description. It follows that in the various SU(3) multiplets the differing accuracy of the model description should be due only to the particular SU(3) symmetry properties of the considered nucleus.

At this point we should mention that the simultaneous fitting of energy levels and transition probabilities is advantageous for our analyses. In order to estimate the significance of such a procedure we refer to the calculations carried out in the framework of the pseudo SU(3) model [19]. In [19] only the ground and γ-band energy levels are used in the fits. The $B(E2)$ transition probabilities are determined using the wave functions obtained from the energy diagonalizations. As a result the energy levels and the gsb intraband transition probabilities of the nuclei $^{160-164}$Dy, $^{164-168}$Er, ^{166,168}Yb, ^{232}Th, and $^{234-238}$U are described satisfactorily. However, the obtained interband transition probabilities (Tables 6 and 7 of [19]) do not reproduce accurately the experimental data. For example, in the case of ^{168}Er, the interband ratio $R_1(L)$ [Eq. (20)] obtains the values $R_1(2)=1.43$, $R_1(4)$

$=3.0$, $R_1(6)=3.72$, while the experimental data give $R_1(2)=1.78$, $R_1(4)=4.81$, $R_1(6)=10.6$ [40,41], i.e., for $L\geqslant 4$ the experimental $R_1(L)$ ratios are not reproduced. Below we shall see that in our calculations (with simultaneous fitting of energy levels and transition probabilities) the same ratio for the same nucleus obtains the values $R_1(2)=1.81$, $R_1(4)=5.34$, $R_1(6)=10.31$, which are in very good agreement with the experimental data. Simultaneous energy $B(E2)$ fits have, in addition, been used in the framework of the pseudosymplectic model [59], the advantages of such a procedure becoming clear also in this case. In addition, we remark that the interband transitions play an important role in our study, since (as will be commented below) they carry information about the coupling of the gsb and γ bands into one SU(3) multiplet.

In the end of this section we should mention that the restriction on the energy levels used in the fits to angular-momentum values up to $L=8-10$ is appropriate because below this limit almost all gsb and γ-band levels of the investigated nuclei are observed experimentally. Such a restriction allows one to study the systematic behavior of the broken SU(3) symmetry in the various nuclei on the basis of the same angular-momentum values. Thus we ensure that in most of the considered nuclei the even-spin levels belonging to the gsb are described together with their γ-band counterparts. The splitting of the even-spin states as well as the band-mixing strengths are then correctly taken into account. An exception is the nucleus ^{238}U for which we consider the gsb up to $L=18$ and the γ band up to $L=5$, due to the lack of further data on the γ band.

IV. RESULTS AND DISCUSSION

A. Nuclei with small SU(3) energy splitting

We have grouped the nuclei under study according to the magnitude of the SU(3) energy splitting. As a measure of the splitting we use the ratio

$$\Delta E_2=(E_{2_2^+}-E_{2_1^+})/E_{2_1^+}, \tag{46}$$

where $E_{2_1^+}$ and $E_{2_2^+}$ are the experimentally measured 2^+ energy levels, belonging to the gsb and the γ band, respectively. In the rare-earth region this ratio varies within the limits $7\leqslant\Delta E_2\leqslant 18$, while in the actinides one observes values in the range $13\leqslant\Delta E_2\leqslant 25$.

We start with the nuclei in which a small band splitting ratio $\Delta E_2\sim 8-10$ is observed. The three Er isotopes $^{164-168}$Er and the nuclei ^{164}Dy and ^{168}Yb are representatives of this group of nuclei. As a typical example let us consider the ^{168}Er case, where $\Delta E_2=9.3$. For this nucleus the model calculations are implemented in the SU(3) irreps within the range $10\leqslant\lambda\leqslant 90$ and $\mu=2,4,6,8$. The results obtained for the description of the energy levels are shown in Fig. 1, where the corresponding rms factors σ_E are plotted as a function of the quantum number λ. One finds that in the $(\lambda,2)$ irreps σ_E exhibits a well-pronounced minimum at $\lambda=20$ with $\sigma_E=3.2$ keV. In the $(\lambda,4)$ irreps the minimum is found at $\lambda=16$, with $\sigma_E=3.8$ keV, while in the $(\lambda,6)$ multiplets it is obtained at $\lambda=14$, with $\sigma_E=5.8$ keV. One also finds that in the $(\lambda,8)$ multiplets σ_E obtains almost constant values,

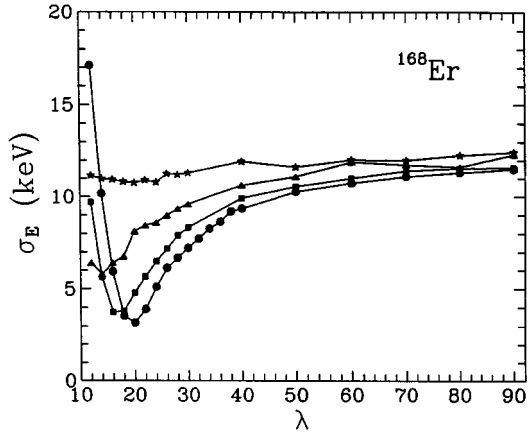

FIG. 1. The energy rms factor σ_E [Eq. (44)], obtained for the nucleus ^{168}Er, is plotted as a function of the quantum number λ at $\mu=2$ (circlets), $\mu=4$ (squares), $\mu=6$ (triangles), and $\mu=8$ (asterisks).

$\sigma_E\sim 11-12$ keV, without the presence of any minimum. Thus, Fig. 1 shows that for ^{168}Er the model scheme provides a clearly outlined region of ''favored'' multiplets in the (λ,μ) plane, including $\lambda=14-20$ and $\mu=2,4,6$. Outside this region σ_E increases gradually with the increase of λ and for $\lambda>40$ it saturates towards the values obtained in the $(\lambda,8)$ multiplets. It is also clear that the best description of the energy levels corresponds to the multiplet (20,2), which provides the absolute σ_E minimum observed in the considered variety of (λ,μ) multiplets (see Table II). In addition, we see that with the increase of the quantum number μ the corresponding σ_E minima increase in value and are shifted to smaller λ values. Regarding the transition probabilities, we remark that the $B(E2)$ ratios [Eqs. (20) and (21)] are reproduced with almost equal accuracy in the whole variety of multiplets, where the rms factor σ_B changes within very narrow limits ($\sigma_B=0.25-0.3$). Actually the differences in the σ_B values obtained in the different multiplets are of the order of the experimental uncertainties. This result is due to the fact that in the present model scheme the $B(E2)$ transition probabilities depend only on the ratio g_3/g_2, which can be adjusted almost equally well in the various irreps. The same behavior of σ_B is observed in all investigated nuclei.

Consider now the parameter values obtained for the nucleus ^{168}Er in the various irreps, plotted in Fig. 2 as a function of the quantum number λ. One sees [Fig. 2(a)] that in the $(\lambda,2)$ multiplets g_1 obtains only positive values which increase gradually with the increase of λ and saturate to $g_1\sim 10$ keV. In the irreps with $\mu=4,6,8$, g_1 starts with negative values [$g_1\sim -13$ keV in the irrep (12,4); $g_1\sim -44$ keV in the irrep (12,8)], but with increasing λ it goes to positive values and saturates towards the values obtained in the $(\lambda,2)$ multiplets. The parameters g_2 and g_3 obtain only negative values, as it is shown in Figs. 2(b) and 2(c). One also finds that both parameters decrease in absolute value with increasing λ and saturate towards zero.

Two comments should be made at this point.

(i) The small g_2 and g_3 absolute values obtained in the large-λ region, $\lambda>40$, do not reduce the respective contributions of the second and the third terms of the Hamiltonian to

TABLE II. The parameters of the fits of the energy levels and the transition ratios [Eqs. (20) and (21)] of the nuclei investigated are listed for the (λ,μ) multiplets which provide the best model descriptions. The Hamiltonian parameters g_1, g_2, and g_3 [Eq. (5)] are given in keV. The quantities σ_E (in keV) and σ_B (dimensionless) represent the energy [Eq. (44)] and the transition [Eq. (45)] rms factors, respectively. The splitting ratios ΔE_2 [Eq. (46), dimensionless] and the vector-boson numbers N [Eq. (9)] are also given.

Nucl	ΔE_2	λ,μ	σ_E	σ_B	g_1	g_2	g_3	N
^{164}Dy	9.4	16,2	14.1	0.52	−1.159	−0.321	−0.590	20
^{164}Er	8.4	18,2	8.1	0.14	3.625	−0.238	−0.513	22
^{166}Er	8.8	16,2	5.8	0.47	2.942	−0.235	−0.572	20
^{168}Er	9.3	20,2	3.2	0.28	4.000	−0.181	−0.401	24
^{168}Yb	10.2	20,2	7.9	0.27	0.500	−0.271	−0.501	24
^{172}Yb	17.6	$\geqslant$80,2	6.8	0.12	9.875	−0.017	−0.052	84
^{176}Hf	14.2	$\geqslant$70,2	15.0	0.17	9.547	−0.030	−0.062	74
^{178}Hf	11.6	34,2	7.0	0.86	8.322	−0.083	−0.213	38
^{238}U	22.6	$\geqslant$60,2	1.6	0.08	−37.697	−0.360	−0.098	64

the energy levels, since the matrix elements of the operators $L\cdot Q\cdot L$ and A^+A increase in absolute value as λ increases (see Table I). Thus one should not consider either $L\cdot Q\cdot L$ or A^+A as small perturbations to the collective rotational energy.

(ii) As a consequence of (i), the diagonal contributions of the terms $L\cdot Q\cdot L$ and A^+A may dominate in the rotational structure of the energy levels. Therefore, the coefficient of the L^2 term, g_1, should not be thought of as the usual inertial parameter. Actually, we have already shown that in the (λ,2) case the inertial term is determined as a linear combination of all of the Hamiltonian parameters [see Eq. (35)]. This is why the negative values of g_1 [as in Fig. 2(a)] should not be considered as a surprise. For example, in the multiplet (16,2) the set of parameters $\{g_1,g_2,g_3\}=\{-1.159,-0.321,-0.590\}$ (given in Table II for the nucleus ^{164}Dy) gives for the inertial term the value $A=11.3$ keV, which is reasonable for nuclei in the rare-earth region.

Furthermore in Fig. 2(d) the ratio g_3/g_2 is plotted as a function of λ. One finds that g_3/g_2 decreases with increasing λ. The change of this ratio compensates for the fact that the A^+A matrix elements increase more rapidly with increasing λ than the matrix elements of the operator $L\cdot Q\cdot L$ (below we shall further discuss the λ dependence of these matrix elements, see also Table I). In such a way the smooth behavior of g_1, g_2, g_3, and g_3/g_2 obtained in the (λ,μ) plane indicates that the present model scheme allows a consistent renormalization of the Hamiltonian parameters for the different SU(3) irreps. For that reason one obtains reasonable model descriptions even in the multiplets outside the favored region.

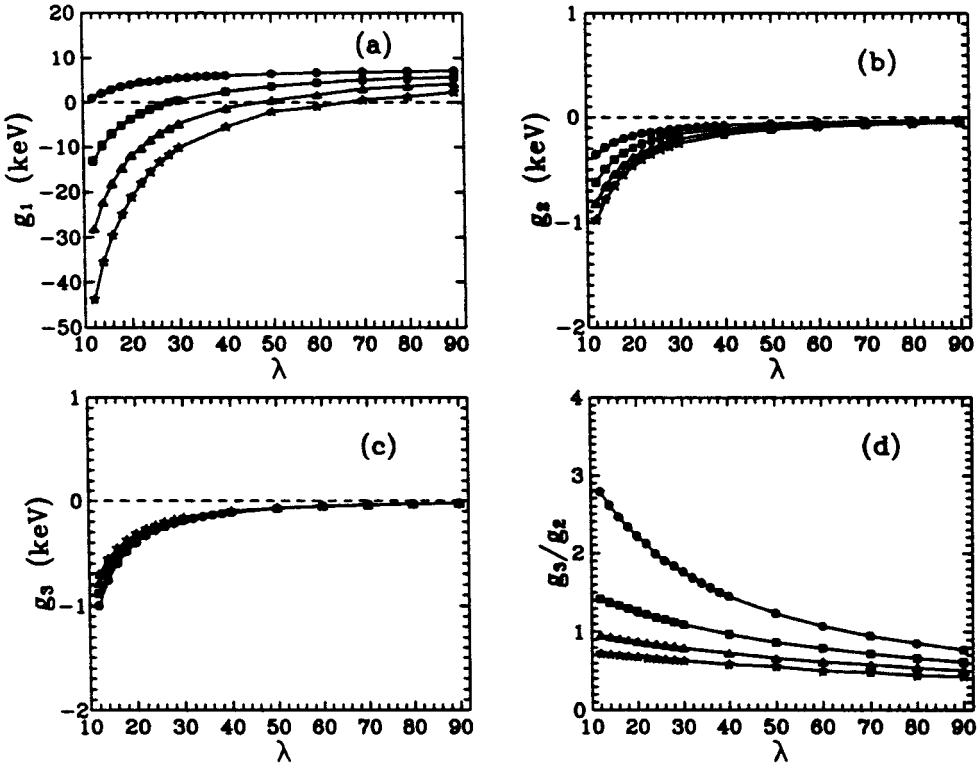

FIG. 2. The Hamiltonian parameters g_1,g_2,g_3 [Eq. (5)] and the ratio g_3/g_2, adjusted for the nucleus ^{168}Er, are plotted [in (a), (b), (c), and (d), respectively] as functions of the quantum number λ at $\mu=2$ (circlets), $\mu=4$ (squares), $\mu=6$ (triangles), and $\mu=8$ (asterisks).

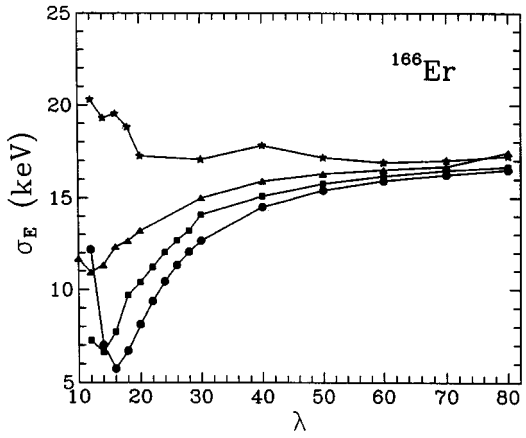

FIG. 3. The same as Fig. 1 but for the nucleus ^{166}Er.

Almost the same picture has been obtained in the other nuclei with small SU(3) energy splittings. For each of them we found a clearly outlined region of favored multiplets as for ^{168}Er. Thus in the ^{168}Er case the favored multiplets are located within the region $\lambda = 12-16$ and $\mu = 2,4,6$, while the best model description is obtained in the irrep (16,2) (see Fig. 3). For the nucleus ^{164}Er the favored multiplets are found within the region $\lambda = 14-18$ and $\mu = 2,4,6$ and the best description corresponds to the irrep (18,2) (see Fig. 4). For the nuclei ^{164}Dy and ^{168}Yb the best model descriptions are established in the multiplets (16,2) and (20,2), respectively [see Figs. 5(a) and 5(b)]. The rms factors σ_E and σ_B and the corresponding values of the parameters obtained in the ''best'' irreps are listed in Table II. We remark that in these irreps very good agreement between theory and experiment is found. Also, we should mention that for all the nuclei considered the parameters of the Hamiltonian exhibit the same numerical behavior in the (λ,μ) plane as the one observed for ^{168}Er.

As a typical example of results given by the broken SU(3) symmetry for nuclei with small SU(3) energy splitting we give in Table III the energy levels and transition ratios calculated for the nuclei ^{164}Dy, $^{164-168}$Er, and ^{168}Yb and compare them to the corresponding experimental data. The parameter values corresponding to these results are the ones given in Table II. Very good agreement between theory and experiment is observed.

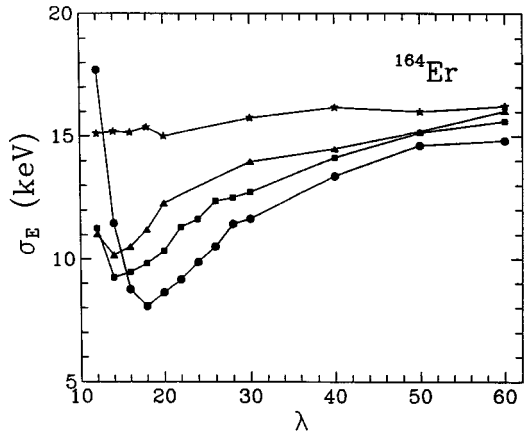

FIG. 4. The same as Fig. 1 but for the nucleus ^{164}Er.

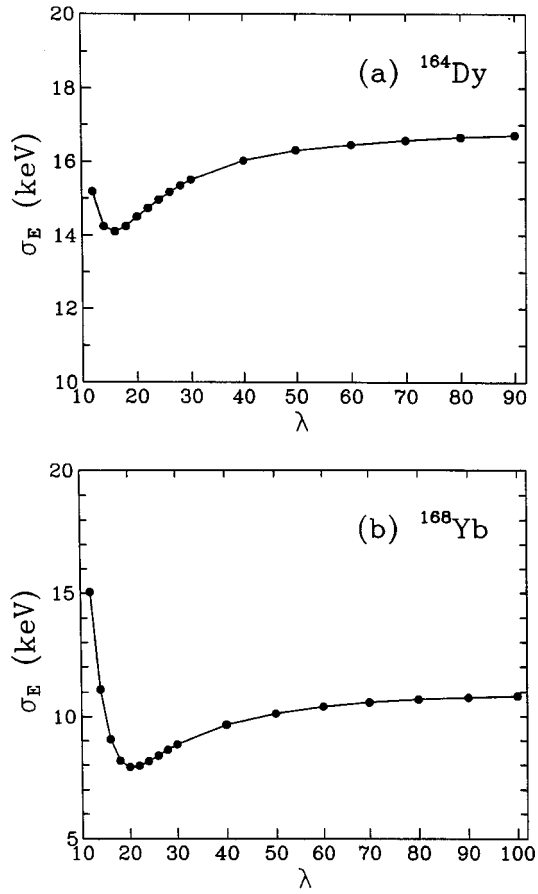

FIG. 5. The energy rms factor σ_E [Eq. (44)], obtained for the nuclei ^{164}Dy and ^{168}Yb [shown in (a) and (b), respectively], is plotted as a function of the quantum number λ at $\mu = 2$.

On the so far presented results the following comments apply.

(i) Although the considered SU(3) scheme allows an appropriate renormalization of the Hamiltonian parameters which leads to reasonable model descriptions in all (λ,μ) multiplets under study, the calculations for the nuclei $^{164-168}$Er clearly outline corresponding regions of favored multiplets, where the descriptions of the energy levels are obtained essentially better than in the other irreps. Since these regions are determined on the basis of the experimental gsb and γ-band characteristics, the above result can be interpreted as a natural physical signature of the broken SU(3) symmetry in these nuclei.

(ii) For the nuclei with small bandsplitting, the best model descriptions are obtained in the multiplets with $\mu = 2$. Generally one finds (see Figs. 1, 3, and 4) that for a fixed quantum number λ the $(\lambda,2)$ irreps give better results than the ones with $\mu > 2$. Note that while the $(\lambda,2)$ multiplets only two bands (the gsb and the γ band), the higher SU(3) irreps with $\mu = 4,6,8,\ldots$ predict the presence of additional higher rotational bands. Thus, for example, the $(\lambda,4)$ multiplets predict an additional rotational band built on a 4^+ state, which in the considered Er isotopes should be observed in the energy region of 3–4 MeV. Indeed in $^{164-168}$Er nuclei such 4^+ states are observed experimentally, but their energies are measured near 2 MeV [56], which excludes the possibility of describing them together with the gsb and the γ bands within

TABLE III. Theoretical and experimental energy levels and transition ratios [Eqs. (20) and (21)] for the nuclei ^{164}Dy, $^{164-168}$Er, and ^{168}Yb. The corresponding (λ,μ) values are also given. The experimental data (used in the fits) for the energy levels are taken from [35], while the data for the $E2$ transitions are from [36–38] (for ^{164}Dy), [38,39] (for ^{164}Er), [40–42] (for ^{166}Er), [43–45] (for ^{168}Er), [45,46] (for ^{168}Yb). The numbers in brackets refer to the uncertainties in the last digits of the experimental ratios.

	Nucleus (λ,μ)											
L	$E_g^{\rm th}$	$E_g^{\rm expt}$	$E_\gamma^{\rm th}$	$E_\gamma^{\rm expt}$	$R_1^{\rm th}$	$R_1^{\rm expt}$	$R_2^{\rm th}$	$R_2^{\rm expt}$	$R_3^{\rm th}$	$R_3^{\rm expt}$	$R_4^{\rm th}$	$R_4^{\rm expt}$
						^{164}Dy (16,2)						
2	71.2	73.4	773.7	761.8	2.13	2.08(40)	0.11	0.082	-	-	-	-
3	-	-	837.9	828.2	-	-	-	-	0.95	0.62	-	-
4	237.2	242.2	924.3	961.0	8.73	9.10	0.26	0.26	-	-	1.39	1.30(17)
5	-	-	1030.5	1024.6	-	-	-	-	2.31	0.83	-	-
6	496.1	501.3	1162.6	1154.0	31.54	-	0.45	-	-	-	1.05	1.14(28)
7	-	-	1309.6	-	-	-	-	-	4.91	-	-	-
8	845.3	843.7	1492.5	-	407.5	-	0.66	-	-	-	0.97	0.97(34)
						^{164}Er (18,2)						
2	86.5	91.4	868.9	860.3	1.88	2.04(31)	0.088	0.11(5)	-	-	-	-
3	-	-	949.2	946.3	-	-	-	-	0.74	0.89(7)	-	-
4	288.0	299.5	1056.6	1058.3	5.92	-	0.20	-	-	-	1.40	1.18(33)
5	-	-	1190.2	1197.5	-	-	-	-	1.52	1.43(13)	-	-
6	604.1	614.4	1352.1	1358.8	12.69	-	0.33	-	-	-	1.06	-
7	-	-	1538.3	1545.1	-	-	-	-	2.65	-	-	-
8	1033.8	1024.6	1756.5	1744.6	29.59	-	0.48	-	-	-	0.98	-
						^{168}Er (16,2)						
2	76.8	80.6	790.9	785.9	1.83	1.86(10)	0.08	0.097(8)	-	-	-	-
3	-	-	860.8	859.3	-	-	-	-	0.70	0.72(6)	-	-
4	255.8	265.0	954.2	956.2	5.47	5.72(47)	0.20	0.26(7)	-	-	1.39	1.45(30)
5	-	-	1070.6	1075.3	-	-	-	-	1.41	1.43(15)	-	-
6	536.6	545.4	1211.4	1215.9	10.72	12.25(75)	0.32	0.28	-	-	1.05	1.12(65)
7	-	-	1373.6	1376.0	-	-	-	-	2.36	-	-	-
8	918.4	911.2	1563.0	1557.7	21.28	20.9(45)	0.48	-	-	-	0.96	1.05(95)
						^{168}Er (20,2)						
2	77.7	79.8	823.7	821.2	1.81	1.78(18)	0.082	0.066(16)	-	-	-	-
3	-	-	896.5	895.8	-	-	-	-	0.68	0.62(6)	-	-
4	258.8	264.1	993.8	994.7	5.34	4.81(78)	0.18	0.078(20)	-	-	1.40	1.53(18)
5	-	-	1115.1	1117.6	-	-	-	-	1.34	1.02(20)	-	-
6	543.1	548.7	1261.6	1263.9	10.31	10.6(20)	0.29	0.19(2)	-	-	1.06	-
7	-	-	1430.9	1432.9	-	-	-	-	2.19	1.62(16)	-	-
8	929.9	928.3	1627.5	1624.5	19.94	-	0.42	-	-	-	0.99	-
						^{168}Yb (20,2)						
2	82.3	87.7	990.0	983.8	1.97	2.06(36)	0.81	0.67(19)	-	-	-	-
3	-	-	1066.3	1066.9	-	-	-	-	0.80	-	-	-
4	273.9	286.6	1168.4	1171.2	6.82	6.72(135)	1.76	1.18(40)	-	-	1.40	-
5	-	-	1295.1	1302.3	-	-	-	-	1.75	-	-	-
6	574.1	585.3	1449.6	1445.1	17.26	17.3(42)	0.36	-	-	-	1.07	-
7	-	-	1624.7	-	-	-	-	-	3.23	-	-	-
8	981.5	970.1	1833.9	-	57.15	-	0.52	-	-	-	1.00	-

the present model scheme. This fact indicates that in the considered nuclei the broken SU(3) symmetry is naturally revealed in the lowest $[(\lambda,2)]$ irreps, where, besides the gsb's and the γ bands, no other bands are predicted. Hence the inclusion of other rotational bands should be implemented by an extension of the present model scheme to a more general DS group, such as Sp(6,$\mathcal{R}$).

(iii) The obtained results can be discussed in terms of the relationship between the collective model shape parameters β, γ [57] and the SU(3) irrep labels (λ,μ) [58]:

$$\beta^2 \sim [\lambda^2+\lambda\mu+\mu^2+3(\lambda+\mu)+3], \tag{47}$$

$$\gamma = \tan^{-1}[\sqrt{3}(\mu+1)/(2\lambda+\mu+3)], \tag{48}$$

where β and γ characterize the axial and the nonaxial quadrupole deformations of the nucleus, respectively. Equations (47) and (48) are derived by requiring a correspondence between the invariants of the triaxial rotor group $T_5 \wedge \mathrm{SO}(3)$ and these of the group SU(3) (for more details see [58]). We should remark that while in [58] the above relationship is considered in a microscopic (shell model) aspect [via (λ,μ)], in the present studies it could be used on a phenomenological level. Thus, we are able to make some estimates for the nuclear quadrupole deformations in terms of the favored SU(3) irreps. As an example consider the favored (λ,μ) region obtained for the nucleus ^{168}Er (Fig. 1). One finds that for the multiplets (20,2), (16,4), and (14,6) Eq. (48) gives $\gamma=6.6°$, $\gamma=12.5°$, $\gamma=18.1°$, respectively. It is clear that the best model description [the multiplet (20,2)] corresponds to relatively small nonaxial deformation of the nucleus. Such estimates can be made for the irreps appearing in the alternative SU(3) models. In the pseudo SU(3) model [19] and in its pseudosymplectic extension [59], the SU(3) irrep used for the nucleus ^{168}Er is (30,8), while in [21] the same nucleus is associated with the multiplet (78,10). We see that although these multiplets lie outside the empirically favored (λ,μ) region, the corresponding values of the angle γ [$\gamma=12.4°$ for (30,8) and $\gamma=6.5°$ for (78,10)] are very close to the ones for (16,4) and (20,2), respectively. We have obtained similar estimates for the other nuclei considered. In all cases we found that the experimental information on the energy levels and the transition probabilities implicitly indicates the presence of small nonaxial deformations.

B. Nuclei with medium and large SU(3) energy splitting

Let us now turn to nuclei in which large band-splitting ratios $\Delta E_2 > 14-15$ are observed. The nuclei ^{172}Yb, ^{176}Hf, and ^{238}U are characterized by such large ΔE_2 values. As a typical example consider the ^{172}Yb case where $\Delta E_2 = 17.6$. In Fig. 6 the rms factors σ_E obtained for this nucleus are given for the (λ,μ) multiplets in the range $10 \leqslant \lambda \leqslant 160$ and $\mu = 2,4,6$. Here, compared with the previously considered nuclei, we find an essentially different picture. We see that in the $(\lambda,2)$ multiplets the σ_E factor, which starts with 29 keV at $\lambda = 12$, decreases with increasing λ and further at $\lambda > 80-90$ saturates gradually to a constant value $\sigma_E \sim 6.5$ keV without reaching any minimum. In the higher irreps with $\mu > 2$, σ_E exhibits almost the same λ dependence and the σ_E values obtained for $\lambda > 80-90$ lie on the average 0.1 keV above the ones obtained in the corresponding $(\lambda,2)$ multiplets. It follows that in the large λ's ($\lambda \sim 100$) all considered multiplets practically provide equally accurate model descriptions. A similar picture is observed in the nuclei ^{176}Hf (with $\Delta E_2 = 14.2$) and ^{238}U (with $\Delta E_2 = 22.6$). This is illustrated in Fig. 7 for the $(\lambda,2)$ multiplets. In ^{176}Hf we found that for large λ values ($\lambda > 70-80$) σ_E saturates to the value $\sigma_E \sim 14.8$ keV [see Fig. 7(a)] and in the nucleus ^{238}U [Fig. 7(b)] σ_E obtains the values $\sigma_E \sim 1.6$ keV (see also Table II). It is clear that in the nuclei with large band splitting the calculations indicate the presence of a wide lower limit of the quantum number λ instead of a narrow region of favored multiplets. Therefore in these nuclei one could make only rough estimates of the nuclear collective characteristics. Thus taking into account that in general $\lambda > 60$ and using Eq. (48) one finds that the strongly splitted SU(3) spectra should correspond to small ($\gamma < 2°$) nonaxial deformations.

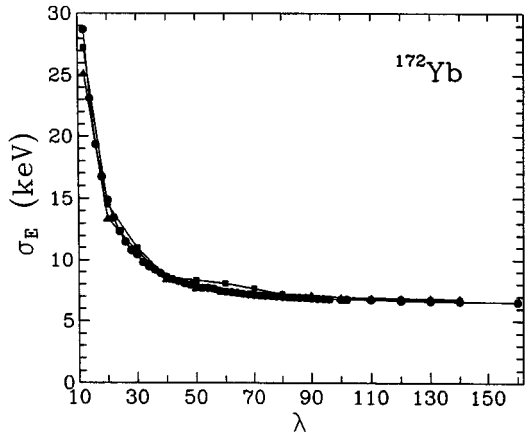

FIG. 6. The energy rms factor σ_E [Eq. (44)], obtained for the nucleus ^{172}Yb, is plotted as a function of the quantum number λ at $\mu = 2$ (circlets), $\mu = 4$ (squares), and $\mu = 6$ (triangles).

It is also interesting to consider the nucleus ^{178}Hf in which one observes a transition value of the band-splitting ratio $\Delta E_2 = 11.6$. In Fig. 8 the σ_E values obtained for this nucleus are plotted for the $(\lambda,2)$ multiplets in the range $10 \leqslant \lambda \leqslant 100$. One sees that σ_E, which starts with the value $\sigma_E \sim 24$ keV at $\lambda = 12$, decreases with increasing λ and in the region $30 \leqslant \lambda \leqslant 40$ obtains a slightly expressed minimum where $\sigma_E \sim 7$ keV. Further on, σ_E increases slowly with λ

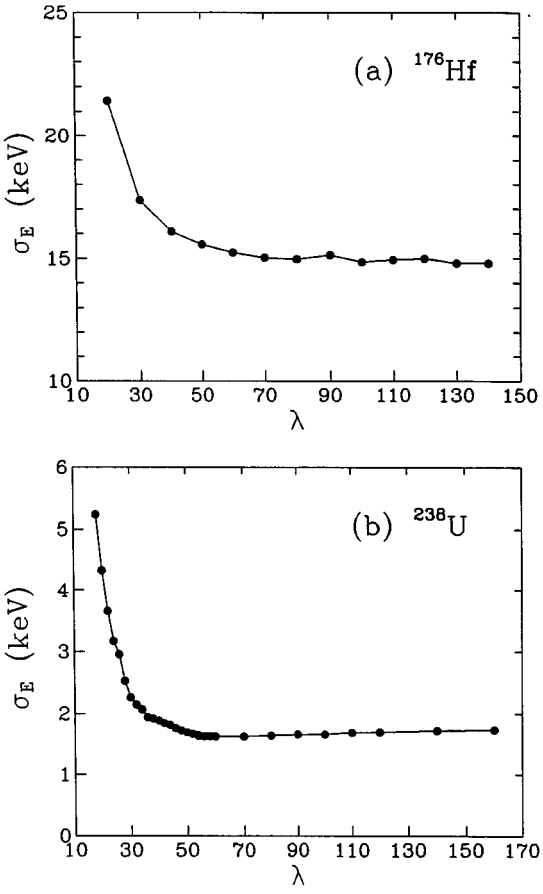

FIG. 7. The same as Fig. 5 but for ^{176}Hf (a) and ^{238}U (b).

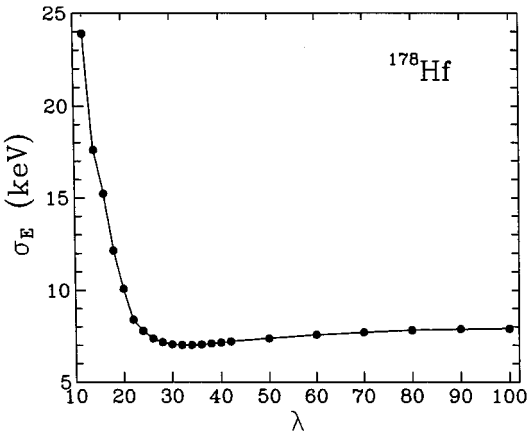

FIG. 8. The same as Fig. 5 but for the nucleus ^{178}Hf.

and near $\lambda=100$ grows up to the value $\sigma_E\sim 8$ keV. Such a result indicates that the global (λ,μ) characteristics of the broken SU(3) symmetry are changed gradually from the nuclei with small band splitting to the nuclei where the splitting is large.

As a typical example of results provided by the broken SU(3) symmetry for nuclei with medium and large SU(3) energy splitting we give in Table IV the energy levels and transition ratios calculated for the nuclei ^{172}Yb, $^{176-178}$Hf, and ^{238}U and compare them to the corresponding experimental data. The parameter values corresponding to these results are the ones given in Table II. Good agreement between theory and experiment is observed.

The following overall picture of the vector-boson model description in deformed nuclei can now be drawn. In the nuclei where the band splitting is small, $\Delta E_2\sim 8-10$ (^{164}Dy, $^{164-168}$Er, ^{168}Yb), the best model descriptions are found in clearly outlined regions of favored (λ,μ) irreps with relatively small values of the quantum number λ $(16\leqslant\lambda\leqslant 20)$ as well as of the quantum number μ $(2\leqslant\mu\leqslant 6)$. Further with the increase of the splitting energy, as in the case of the nucleus ^{178}Hf (with $\Delta E_2=11.6$), the favored multiplets are shifted gradually to larger λ values ($\lambda\sim 40$) with slightly expressed σ_E minimum. In the nuclei where large band splitting is observed, $\Delta E_2\sim 14-22$ (^{172}Yb, ^{176}Hf, ^{238}U), the present theoretical scheme provides almost equally good model descriptions in all (λ,μ) multiplets with $\lambda>60$ up to $\lambda=160$ and $\mu=6$. The estimates of the shape parameters show that the increasing magnitude of SU(3) splitting indicates an increase in the axial [β, Eq. (47)] and decrease in the nonaxial [γ, Eq. (48)] deformations of nuclei.

C. Band-mixing interactions

The above picture can be analyzed in terms of the collective SU(3) Hamiltonian and the respective band-mixing interactions. For this purpose we study the λ dependence of the Hamiltonian matrix elements and estimate their contribution to the energy spectrum in the large-λ limit. (Since the physically significant values of the quantum number μ do not exceed $\mu=8-10$, the large-μ limit is of no practical interest.)

Let us consider the case of the $(\lambda,2)$ multiplets (without restriction on the higher irreps) where in the even-spin states the dimension of the Hamiltonian matrix is $d_L=2$. From the analytical expressions given in Table I and Eqs. (27)–(30) we can estimate the λ dependence of the total contribution of the second and third terms of the Hamiltonian, $L\cdot Q\cdot L$ and A^+A, in the diagonal and off-diagonal matrix elements. In the large-λ limit the diagonal matrix elements $V_{1,1}$ and $V_{2,2}$ increase in absolute value, with the increasing of λ, as λ and λ^2, respectively. The lower off-diagonal matrix element $V_{2,1}$ increases as λ^2, while the upper one, $V_{1,2}$, does not depend on λ. Hence the total contribution of the diagonal matrix elements in the eigenvalue equation (12) increases as λ^3, while the total contribution of the off-diagonal ones increases as λ^2. It follows then that in the large-λ limit the relative contribution of the off-diagonal (band-mixing) matrix elements of the operators $L\cdot Q\cdot L$ and A^+A (compared to the diagonal ones) decreases as $1/\lambda$. We note that in the case of multiplets with $\mu>2$ this contribution decreases even more rapidly.

The above estimates show that the increase in the quantum number λ is connected with the corresponding decrease in the mixing interaction between the gsb and the γ band within the framework of the SU(3) symmetry. Hence for the nuclei with small band splitting (^{164}Dy, $^{164-168}$Er, ^{168}Yb) the relatively small λ values ($\lambda\sim 16-20$) indicate that the gsb and the γ bands are strongly mixed. In the nuclei with a large band splitting (^{172}Yb, ^{176}Hf, ^{238}U) the large λ's correspond to a weak interaction between the two bands. This means that for the latter nuclei the rotational character of the gsb and the γ bands should be better developed. Indeed the case of the nucleus ^{238}U with a very large splitting ratio $\Delta E_2=22.6$ and a well-pronounced rotational structure of the gsb supports the above supposition.

The obtained (λ,μ) characteristics of deformed nuclei allow one to gain a physical insight into the vector-boson realization of a broken SU(3) symmetry. To illustrate this, we refer to the number of vector bosons N determined for a given (λ,μ) multiplet through Eq. (9). We see that our results give a possibility to estimate the number N for the nuclei under study. Thus we find that in the cases of small band splitting the favored (λ,μ) regions imply relatively small vector-boson numbers $N\sim 20-30$, while for the strongly splitted SU(3) spectra one has $N\sim 80-100$. Then taking into account the λ dependence of the Hamiltonian matrix elements one deduces that the increase of N can be connected to the decrease in the band-mixing interaction. In these terms the large-λ limit ($\lambda\rightarrow\infty$) boils down to the limit $N\rightarrow\infty$, which corresponds to an asymptotical decrease of the band interaction to zero. Thereby the multiplet splits into distinct noninteracting rotational bands and the SU(3) symmetry gradually disappears. This situation is equivalent to the group contraction process in which the SU(3) algebra reduces to the algebra of $T_5\wedge$SO(3) [58]. In such a way the SU(3) symmetry goes to that of the rotator. Note that an analogous transition is inherent in the IBM [14] and corresponds to an infinite number of bosons. However one should not make any analogy between the s and d bosons of the IBM and the vector bosons since the latter are introduced as quanta of elementary collective excitations and cannot be treated as coupled nucleon pairs.

TABLE IV. The same as Table III but for the nuclei ^{172}Yb, ^{176}Hf, ^{178}Hf, ^{238}U. The experimental data for the energy levels are taken from [35], while the data for the $E2$ transitions are from [47–49] (for ^{172}Yb), [50,51] (for ^{176}Hf), [52,53] (for ^{178}Hf), [54] (for ^{238}U).

					Nucleus (λ,μ)							
L	$E_g^{\rm th}$	$E_g^{\rm expt}$	$E_\gamma^{\rm th}$	$E_\gamma^{\rm expt}$	$R_1^{\rm th}$	$R_1^{\rm expt}$	$R_2^{\rm th}$	$R_2^{\rm expt}$	$R_3^{\rm th}$	$R_3^{\rm expt}$	$R_4^{\rm th}$	$R_4^{\rm expt}$
					^{172}Yb $(\geqslant 80,2)$							
2	76.5	78.7	1480.4	1465.7	1.50	1.60(22)	0.05	0.105(13)	-	-	-	-
3	-	-	1556.2	1549.2	-	-	-	-	0.43	0.50(6)	-	-
4	256.0	260.1	1657.4	1657.9	3.18	3.12(48)	0.10	-	-	-	1.43	1.61(31)
5	-	-	1783.8	1792.3	-	-	-	-	0.65	-	-	-
6	535.5	539.8	1933.3	-	4.22	-	0.13	-	-	-	1.10	0.98(41)
7	-	-	2111.3	-	-	-	-	-	0.79	-	-	-
8	917.9	911.3	2314.8	-	4.97	-	0.15	-	-	-	1.04	1.20(47)
					^{176}Hf $(\geqslant 70,2)$							
2	84.2	88.4	1361.4	1341.3	1.54	1.28(21)	0.06	0.13(5)	-	-	-	-
3	-	-	1444.9	1445.8	-	-	-	-	0.48	0.61(23)	-	-
4	280.8	290.2	1556.2	1540.2	3.56	-	0.11	-	-	-	1.43	-
5	-	-	1695.3	1727.7	-	-	-	-	0.76	-	-	-
6	589.6	597.0	1862.3	1861.9	5.04	-	0.15	-	-	-	1.10	-
7	-	-	2047.6	-	-	-	-	-	0.99	-	-	-
8	1010.7	998.0	2270.0	-	6.40	-	0.19	-	-	-	1.04	-
					^{178}Hf (34,2)							
2	88.9	93.2	1180.2	1174.8	1.60	1.63(22)	0.06	0.11(6)	-	-	-	-
3	-	-	1266.6	1268.9	-	-	-	-	0.51	0.46(8)	-	-
4	296.4	306.6	1381.8	1384.6	3.84	5.9(10)	0.13	0.29(8)	-	-	1.42	-
5	-	-	1525.7	1533.6	-	-	-	-	0.86	0.66(26)	-	-
6	622.5	632.2	1698.5	1691.4	5.71	4.76(210)	0.18	-	-	-	1.09	-
7	-	-	1899.0	-	-	-	-	-	1.16	-	-	-
8	1067.0	1058.6	2129.2	-	7.61	-	0.23	-	-	-	1.03	-
					^{238}U $(\geqslant 60,2)$							
2	44.9	44.9	1062.2	1060.3	5.83	-	0.24	-	-	-	-	-
3	-	-	1105.9	1105.7	-	-	-	-	4.57	-	-	-
4	148.6	148.4	1165.9	1168.0	92.66	-	0.69	-	-	-	1.43	-
5	-	-	1235.2	-	-	-	-	-	91.86	-	-	-
6	308.1	307.2	1329.9	-	5.14	-	1.25	-	-	-	1.10	-
7	-	-	1425.2	-	-	-	-	-	114.5	-	-	-
8	519.4	518.3	1563.1	-	1.83	-	1.80	-	-	-	1.04	-
9	-	-	1673.8	-	-	-	-	-	19.41	-	-	-
10	777.1	775.7	1868.3	-	1.00	-	2.25	-	-	-	1.02	1.17(110)
12	1076.5	1076.5	-	-	-	-	-	-	-	-	1.01	1.11(125)
14	1413.4	1415.3	-	-	-	-	-	-	-	-	1.00	0.93(118)
16	1785.9	1788.2	-	-	-	-	-	-	-	-	1.00	1.00(68)
18	2193.9	2190.7	-	-	-	-	-	-	-	-	1.00	0.98(65)

D. Discussion

The so far presented results and analyses allow us to discuss the applicability and the limitations of the broken SU(3) symmetry in nuclei. In addition the relevance of the gsb–γ-band coupling scheme can be clarified in terms of the investigated SU(3) multiplets. First, consider the weakly splitted spectra. In these cases the established regions of favored (λ,μ) irreps suggest a cutoff in the gsb near $L=16-20$, which in general is in agreement with the experimental picture observed in rare-earth nuclei. We note that since the present model is addressed to the low-lying spectra (below the backbending), one should not try to discuss the higher-energy levels (in our studies we consider the gsb and not the yrast band). On the other hand, the narrow limits of the favored regions suggest relatively well-determined values of the shape characteristics (β,γ). These considerations indicate that for the nuclei with $\Delta E_2 \sim 8-10$, both the gsb and the γ band are united into one SU(3) multiplet in a consistent way. In the strongly split spectra the situation is quite different. The lack of any upper limit for the quantum number λ suggests the presence of high angular momenta $L \sim 60-80$ which are not reasonable in the low-spin regime of nuclear collective motion. For the same reason one could not obtain clear estimates for the nuclear shape parameters as in the cases of favored (λ,μ) regions. Furthermore, the large λ values correspond to excessively large (Pauli forbidden) axial

deformations of nuclei [see Eq. (47)]. The above facts show that for nuclei with a large splitting ratio $\Delta E_2 > 14$ the gsb–γ-band coupling scheme comes up against basic difficulties in the consistent treatment of nuclear collective characteristics. At least these nuclei should be referred to the limiting case in which the two bands are weakly coupled in the framework of one SU(3) multiplet. This is a worth-mentioning finding which could be interpreted as an indication for a possible rearrangement of the collective rotational bands in different SU(3) irreps. We can point out two experimental pieces of evidence supporting this supposition.

(i) For the nuclei with a large 2^+ splitting the number of the experimentally observed gsb–γ-interband transitions is essentially smaller than the one in the nuclei where ΔE_2 is small. Moreover in the nucleus ^{238}U such transitions have not been observed.

(ii) Consider the mutual disposition of the second 2^+ collective levels $E_{2_2^+}$ (the γ-band bandhead) and the corresponding second 0^+ levels $E_{0_2^+}$ (the β-band bandhead) of rotational nuclei [35]. Note that for the nuclei with small ΔE_2 (^{164}Dy, $^{164-168}$Er, ^{168}Yb) one observes $E_{2_2^+} < E_{0_2^+}$ (for example, for ^{168}Er one has $E_{2_2^+} = 0.821$ MeV and $E_{0_2^+} = 1.217$ MeV). For the nucleus ^{178}Hf, which has a transitional ΔE_2 value, both energies are almost equal ($E_{2_2^+} = 1.175$ MeV, $E_{0_2^+} = 1.199$ MeV). For the nuclei with large 2^+ splitting (^{172}Yb, ^{176}Hf, ^{238}U) one finds $E_{2_2^+} > E_{0_2^+}$ (for example, for ^{172}Yb one has $E_{2_2^+} = 1.466$ MeV and $E_{0_2^+} = 1.042$ MeV). The latter observation indicates that in the nuclei with $\Delta E_2 > 14$ the gsb and the γ band could be situated in distinct SU(3) multiplets.

We remark that our analysis is consistent with the results obtained for the nucleus ^{238}U in the framework of the pseudo SU(3) and pseudo symplectic schemes [19,59]. It is shown that the ''leading'' irrep appearing for this nucleus is (54,0), which indicates that in this case the gsb probably belongs to a separate irrep. Actually, the obtained systematic properties of the SU(3) symmetry in deformed nuclei could be interpreted as the manifestation of a more general DS in nuclear collective motion. In this respect the gsb–γ-band coupling schemes and the IBM collective scheme could be considered rather as complementary than as alternative schemes. The dynamical mechanism causing the rearrangement of rotational bands in the various SU(3) irreps could receive attention in the framework of a larger DS group.

A more detailed comparison between the features of the present scheme and these of the interacting boson model (IBM) is now in place. As has already been mentioned, in IBM the lowest γ and β bands belong to the same SU(3) irrep $(2N-4,2)$, while the gsb remains alone in the most symmetric irrep $(2N,0)$ (where N is the total number of active bosons). Formally both band coupling schemes, the gsb-γ scheme (of the present model) and β-γ scheme (of IBM) could be referred to SU(3) multiplets of the type $(\lambda,2)$. However, in the exact SU(3) limit of the original IBM-1 [14] the appearing $(\lambda,2)$ multiplets are degenerate with respect to the Elliott quantum number K. This degeneracy (which is generally in disagreement with the experimental situation) can be removed in several ways. One possible way is to break the exact SU(3) symmetry. This can be achieved (see [24] and references therein) by using in the usual IBM-1 Hamiltonian of the SU(3) limit

$$H_{\mathrm{SU}(3)} = -\kappa(Q\cdot Q) + \kappa'(L\cdot L), \tag{49}$$

the operator

$$Q_m = (d^+\tilde{s} + s^+\tilde{d})^2_m + \chi(d^+\otimes\tilde{d})^2_m, \tag{50}$$

where κ and κ' are the model parameters, and s^+, d^+ (s,d) are the creation (annihilation) operators for the s and d bosons, with $\tilde{s}=s$ and $\tilde{d}_m = (-1)^m d_{-m}$. In the case of $\chi = -\sqrt{7}/2, Q$ is a generator of SU(3) and the exact SU(3) Hamiltonian is obtained. If $\chi = 0$, Q is a generator of O(6) and the Hamiltonian of Eq. (49) is not an SU(3) Hamiltonian anymore. The case $-\sqrt{7}/2 < Q < 0$ corresponds to a broken SU(3) symmetry. The β and γ bands then belong to one splitted $(\lambda,2)$ multiplet. In such a way the β-γ band coupling scheme of the IBM becomes very similar to the present gsb-γ scheme.

The same problem can also be solved by adding to $H_{\mathrm{SU}(3)}$ some higher-order interaction terms. Such a term is the so-called O(3) scalar shift operator which corresponds to a three-body interaction [60]. This operator, usually denoted by Ω, possesses a realization in terms of s and d bosons and is equivalent to the second term of the vector-boson Hamiltonian [Eq. (5)]. It is not diagonal in the Elliot basis [1], its eigenvalues in the $(\lambda,2)$ irreps being [60]

$$\langle\Omega\rangle = \sqrt{6}[L(L+1)-12](2\lambda+5), \quad L=\text{odd}, \tag{51}$$

$$\langle\Omega\rangle = \sqrt{6}\{(L-2)(L+3)(2\lambda+5) \pm 6\sqrt{L(L+1)(L-1)(L+2)+(2\lambda+5)^2}\}, \quad L=\text{even}, \tag{52}$$

with $\langle\Omega\rangle = 0$ for $L=0$. The double sign in Eq. (52) breaks the degeneracy between the levels of the β and γ bands and thus the multiplet is splitted. Again we find that the situation is very similar to that of the present SU(3) symmetry model. Moreover, if we consider the vector-boson Hamiltonian [Eq. (5)] with $g_2 = 1$ and $g_3 = 0$, the square-root terms of Eqs. (32) and (33) coincide exactly with the square-root term in Eq. (52). Thus in this case the β-γ band coupling scheme of the IBM and the gsb-γ scheme of the present model are characterized by the same analytical expression for the energy splitting:

$$|E_\gamma(L) - E_\nu(L)| \sim \sqrt{f(L)+(2\lambda+5)^2}, \quad L=\text{even}, \tag{53}$$

where ν labels the gsb (in the present model) or the β band (in IBM), and $f(L)$ is defined in Eq. (39). Note that while in the gsb-γ scheme the $(+)$ sign in Eq. (52) always corresponds to the γ band and the $(-)$ sign always corresponds to the gsb (i.e., the gsb levels are always below the respective γ-band levels), in the β-γ scheme the $\pm$ correspondence depends on the mutual displacement of the levels and may be changed.

A comment concerning the transition probabilities in the vector-boson model and in the IBM can be made here. While

in the first model the γ-gsb interband $E2$ transitions are naturally incorporated, in the second one [in the exact SU(3) limit] they are forbidden. This type of transition can be allowed in IBM by modifying the quadrupole transition operator similarly to Eq. (50), i.e., by breaking the exact SU(3) symmetry (see [24] and references therein).

It should also be mentioned that the large λ values appearing in our work for the nuclei with large ΔE_2 splitting correspond to the large λ values obtained with the introduction of g bosons in the framework of the sdg-IBM [61,62], where the band cutoffs are shifted towards higher angular momenta.

The above considerations illustrate some differences between the present model and the IBM, as well as some common schematic features of both models. The present analysis also allows one to estimate the relative appropriateness of these model schemes for a particular rotational nucleus or group of nuclei. Our results suggest that for nuclei with small ΔE_2 splitting ratio the gsb-γ band coupling scheme of the vector-boson model is more appropriate than the β-γ scheme of IBM. As a typical example for this case we consider the nucleus ^{168}Er, in which a large number of γ-gsb interband $E2$ transitions are observed [40–42]. For the nuclei with large gsb-γ splitting the β-γ coupling scheme of IBM seems to be more appropriate. As a typical example for this case we consider the nucleus ^{238}U.

In conclusion, the indicated rearrangement of the rotational bands in various SU(3) multiplets can be interpreted as an interplay between the different DS schemes of the vector-boson model and the IBM. The dynamical mechanism causing this rearrangement should be considered in the framework of the DS of a group larger than SU(3).

V. CONCLUSIONS

In this paper we have studied the broken SU(3) symmetry in deformed even-even nuclei via the formalism of the collective vector-boson model. We assume that the physically meaningful properties of this symmetry are developed in certain regions of (λ,μ) irreps, instead of one fixed irrep. In this way there is no microscopic input in the determination of the (λ,μ) irrep of SU(3) suitable for each nucleus, the quantum numbers λ and μ being treated as free parameters and fitted to the experimental data. The available experimental information on energy levels and transition probabilities allows one to identify two kinds of nuclei with SU(3) symmetry.

(i) The nuclei with weak 2^+ splitting [$\Delta E_2 < 12$, defined in Eq. (24)], for which we obtain narrow regions of favored SU(3) irreps (in general one has $16 \leqslant \lambda \leqslant 20$ and $2 \leqslant \mu \leqslant 6$). In these regions the gsb-γ band coupling scheme gives good model estimates of the nuclear collective characteristics under study.

(ii) The nuclei with strong 2^+ splitting [$\Delta E_2 > 12$, defined in Eq. (24)], for which the successful model description requires large values of the quantum number λ ($\lambda > 60-80$) without any presence of particular regions of favored irreps. In these nuclei the applied SU(3) scheme allows only rough estimates of nuclear collective properties. These nuclei are very good rotators, so that a pure SU(3) scheme, like the one of IBM, appears as more appropriate.

In such a way we find that the violation of the SU(3) symmetry, measured by the splitting ratio ΔE_2 [defined in Eq. (24)], determines to a great extent the most important SU(3) properties of deformed nuclei.

A systematic analysis of the gsb-γ band-mixing interaction on the basis of the collective vector-boson model leads to the following conclusions: Increasing number of vector bosons N corresponds to the increase in the splitting of the multiplet and leads to decrease in the band-mixing interaction within the framework of the SU(3) symmetry. In these terms the large-λ limit corresponds to $N \rightarrow \infty$ and has the meaning of SU(3) group contraction. In the limiting case the SU(3) symmetry is completely destroyed and the bands cannot be united anymore in one SU(3) multiplet. Following the above analysis, we conclude that the strongly split spectra should be considered as special cases in which the gsb and the γ bands are weakly coupled. Furthermore the experimental and theoretical examples given for these spectra indicate the possibility for rearrangement of the two bands into distinct irreps. This finding suggests the presence of a transition from the gsb-γ band coupling scheme (in the nuclei with small ΔE_2) to an alternative collective scheme (in the cases of large ΔE_2), in which the gsb is situated in a separate irrep. In other words the broken SU(3) scheme is favored in the case of weak 2^+ splitting, while strong 2^+ splitting favors SU(3) schemes like the one of the IBM, in which the gsb is situated in a separate irrep.

The collective dynamical mechanism causing such a transition from the broken SU(3) of the present model to the pure SU(3) of the IBM could be sought in the framework of the more general DS group Sp(6,$\mathcal{R}$). In such a framework the lowest β-band, absent from the broken SU(3) model considered here, could be included, belonging to an irrep different from the one in which the gsb and the lowest γ band are located. These will be the subjects of a future investigation.

ACKNOWLEDGMENTS

The authors are thankful to S. Pittel for illuminating discussions and for a careful reading of the manuscript. This work was supported in part by the Bulgarian National Fund for Scientific Research under Contract Nos. F-547 and F-415. One of the authors (D.B.) was supported by the EU under Contract No. ERBCHBGCT930467 and by the Greek General Secretariat of Research and Technology under Contract No. PENED95/1981. Another author (P.P.R.) was supported by the Istituto Nazionale di Fisica Nucleare (INFN) and the Italian Ministero dell' Università e della Ricerca Scientifica e Tecnologica (MURST).

[1] J. P. Elliott, Proc. R. Soc. London, Ser. A **245**, 128 (1958); **245**, 562 (1958); J. P. Elliott and M Harvey, *ibid.* **272**, 557 (1963).

[2] R. F. Dashen and M. Gell-Mann, Phys. Lett. **17**, 142 (1965).

[3] L. Weaver and L. C. Biedenharn, Phys. Rev. Lett. **32B**, 326 (1970).

[4] P. P. Raychev, Sov. J. Nucl. Phys. **16**, 643 (1972).

[5] G. Afanasjev and P. Raychev, Part. Nuclei **3**, 436 (1972).

[6] P. P. Raychev and R. P. Roussev, Sov. J. Nucl. Phys. **27**, 1501 (1978).
[7] G. Rosensteel and D. J. Rowe, Ann. Phys. (N.Y.) **96**, 1 (1976).
[8] G. Rosensteel and D. J. Rowe, Phys. Rev. Lett. **38**, 10 (1977).
[9] G. Rosensteel and D. J. Rowe, Ann. Phys. (N.Y.) **104**, 134 (1977).
[10] G. Rosensteel and D. J. Rowe, Ann. Phys. (N.Y.) **126**, 343 (1980).
[11] G. F. Filippov, V. I. Ovcharenko, and Yu. F. Smirnov, *Microscopic Theory of Nuclear Collective Excitations* (Naukova Dumka, Kiev, 1981).
[12] A. Arima and F. Iachello, Phys. Rev. Lett. **35**, 1069 (1975).
[13] A. Arima and F. Iachello, Ann. Phys. (N.Y.) **99**, 253 (1976).
[14] A. Arima and F. Iachello, Ann. Phys. (N.Y.) **111**, 201 (1978).
[15] A. Arima and F. Iachello, Ann. Phys. (N.Y.) **123**, 468 (1979).
[16] F. Iachello and A. Arima, *The Interacting Boson Model* (Cambridge University Press, Cambridge, 1987).
[17] C. L. Wu, D. H. Feng, X. G. Chen, J. Q. Chen, and M. W. Guidry, Phys. Lett. **168B**, 313 (1986).
[18] C. L. Wu, D. H. Feng, X. G. Chen, J. Q. Chen, and M. W. Guidry, Phys. Rev. C **36**, 1157 (1987).
[19] J. P. Draayer and K. J. Weeks, Ann. Phys. (N.Y.) **156**, 41 (1984).
[20] R. M. Asherova, V. I. Ovcharenko, Yu. F. Smirnov, and G. F. Filippov, Izv. Akad. Nauk SSSR, Ser. Fiz. **47**, 957 (1983).
[21] R. M. Asherova, Yu. F. Smirnov, and G. F. Filippov, Obninsk Report IPE-1958, 1989.
[22] S. Alisauskas, P. P. Raychev, and R. P. Roussev, J. Phys. G **7**, 1213 (1981).
[23] P. P. Raychev and R. P. Roussev, J. Phys. G **7**, 1227 (1981).
[24] D. Bonatsos, *Interacting Boson Models of Nuclear Structure* (Clarendon, Oxford, 1988).
[25] L. C. Biedenharn and J. D. Louck, *Encyclopedia of Mathematics and its Applications* (Addison-Wesley, Reading, MA, 1981), Vol. 8.
[26] L. C. Biedenharn, J. Phys. A **22**, L873 (1989).
[27] A. J. Macfarlane, J. Phys. A **22**, 4581 (1989).
[28] V. Bargmann and M. Moshinsky, Nucl. Phys. **23**, 177 (1961).
[29] M. Moshinsky, J. Patera, R. T. Sharp, and P. Winternitz, Ann. Phys. (N.Y.) **95**, 139 (1975).
[30] B. R. Judd, W. Miller, J. Patera, and P. Winternitz, J. Math. Phys. (N.Y.) **15**, 1787 (1974).
[31] P. P. Raychev, R. P. Roussev, and Yu. F. Smirnov, J. Phys. A **24**, 2943 (1991).
[32] G. N. Afanasjev, S. A. Avramov, and P. P. Raychev, Sov. J. Nucl. Phys. **16**, 53 (1972).
[33] M. A. J. Mariscotti, G. Scharff-Goldhaber, and B. Buck, Phys. Rev. **178**, 1864 (1969).
[34] W. H. Press, B. P. Flannery, S. A. Teukolsky, and W. T. Vetterling, *Numerical Recipes* (Cambridge University Press, Cambridge, 1986), p. 294.
[35] M. Sakai, At. Data Nucl. Data Tables **31**, 399 (1984).
[36] E. P. Grigoriev and V. G. Soloviev, *Structure of Even Deformed Nuclei* (Nauka, Moscow, 1977).
[37] S. C. Gujrathi and J. M. D'Auria, Nucl. Phys. **A172**, 353 (1971).
[38] E. N. Shurshikov, Nucl. Data Sheets **47**, 433 (1986).
[39] F. W. N. de Boer, P. F. A. Goudsmit, P. Koldlwiji, and B. J. Meijer, Nucl. Phys. **A169**, 577 (1971).
[40] C. W. Reich and J. E. Gline, Nucl. Phys. **A159**, 181 (1970).
[41] C. W. Reich and J. E. Gline, Phys. Rev. **129**, 2152 (1963).
[42] A. E. Ignatochkin, E. N. Shurshikov, and Yu. F. Jaborov, Nucl. Data Sheets **52**, 365 (1987).
[43] P. E. Hanstein and A. B. Tucker, Nucl. Phys. **A173**, 321 (1971).
[44] H. R. Koch, Z. Phys. **192**, 142 (1966).
[45] V. S. Shirley, Nucl. Data Sheets **53**, 223 (1988).
[46] A. Charvet, R. Duffait, A. Emsallem, and R. Chery, Nucl. Phys. **A156**, 276 (1970).
[47] K. Wien, Z. Phys. **216**, 1 (1968).
[48] D. Sen and E. F. Zganjar, Nucl. Phys. **A145**, 634 (1970).
[49] G. Wang, Nucl. Data Sheets **51**, 577 (1985).
[50] R. Broda, V. Vales, I. Zvolsky, I. Molnar, N. Nenov, E. Z. Rindina, U. M. Fainery, and P. Shoshev, Izv. Akad. Nauk SSSR, Ser. Fiz. **35**, 707 (1971).
[51] E. Browne, Nucl. Data Sheets **60**, 227 (1990).
[52] B. Fogelberg and A. Baclin, Nucl. Phys. **A171**, 353 (1971).
[53] E. Browne, Nucl. Data Sheets **54**, 199 (1988).
[54] E. N. Shurshikov, Nucl. Data Sheets **53**, 601 (1988).
[55] L. Aleksandrov, Math. Phys. Comput. Math. **11**, 36 (1971); JINR Dubna Report BI-5-9969, 1976 (unpublished).
[56] P. C. Sood, D. M. Headly, and R. K. Sheline, At. Data Nucl. Data Tables **47**, 89 (1991).
[57] A. Bohr and B. R. Mottelson, *Nuclear Structure* (Benjamin, New York, 1975), Vol. II.
[58] J. P. Draayer, in *Algebraic Approaches to Nuclear Structure: Interacting Boson and Fermion Models*, Contemporary Concepts in Physics VI, edited by R. F. Casten (Harwood, Chur, 1993), p. 423.
[59] D. Troltenier, J. P. Draayer, P. O. Hess, and O. Castaños, Nucl. Phys. **A576**, 351 (1994).
[60] G. Van den Berghe, H. E. De Meyer, and P. Van Isacker, Phys. Rev. C **32**, 1049 (1985).
[61] H. C. Wu, Phys. Lett. **110B**, 1 (1982).
[62] Y. Akiyama, Nucl. Phys. **A433**, 369 (1985).